Detecting Protein−Protein Interactions by Isotope-Edited Infrared Spectroscopy: A Numerical Approach

Fabian Zehender, Andreas Labahn, and Thorsten Koslowski*

Institut für Physikalische Chemie, Universität Freiburg, Albertstrasse 23a, D-79104 Freiburg im Breisgau, Germany

Received: June 27, 2005; In Final Form: October 16, 2005

We present a theoretical and numerical analysis of the vibrational coupling between isotope-edited amino acids in protein dimers. Depending on the presence and magnitude of coupling between $^{13}C_\alpha$═O peptide bond oscillators, characteristic level splittings of vibrational eigenstates are predicted. For the example of the Gramicidin A ion channel polypeptide, we observe typical IR fingerprints for the head-to-head and the antiparallel double-helical conformation of the dimer. We suggest that these findings can be used to clearly identify the structure of polypeptide aggregates using a particularly simple isotope substitution pattern.

1. Introduction

Infrared spectroscopy is an important analytical tool in biophysics and biochemistry: the vast majority of biologically relevant macromolecules like proteins, phospholipids, and polynucleotides show characteristic IR bands that permit their study in an aqueous environment, including in vivo experiments.[1] In the past decade, isotope substitution has become an important technique in biochemical applications of infrared spectroscopy. Isotope-edited building blocks of the molecules of life are now commercially available, and a constant progress in protein and DNA synthesis permits the introduction of a deuterium, ^{13}C, ^{18}O, or ^{15}N label in a variety of comparatively large molecules. For proteins, isotope substitution can be achieved according to the following strategies: the introduction of labeled precursors into a metabolic pathway,[2] de novo protein synthesis,[3,4] cell-free protein synthesis with a modified suppressor tRNA,[5] or an eukaryotic cell-free translational system.[6]

As detailed below, a change of a single atomic mass implies an altered IR spectrum in a chemically intact environment. To detect small changes in the spectra upon substitution, the technique of Fourier transformed infrared (FTIR) difference spectroscopy[7] has become particularly useful. Sample applications include the use of a deuterated methionine methyl group as a probe of the reduction state and chemical environment of the Fe ion within cytochrome *c* and its mutants.[8] Furthermore, deuteration has been used to study the conformational analysis of alkylamino chains[9] and nucleosides,[10] protein−lipid interactions,[11−14] and the conformation of membrane proteins.[4] Work on the application of single and multiple ^{13}C isotope substitution has focused on the determination of the secondary structure of proteins and peptides.[15−20] In the past couple of years, theoretical and computational chemistry approaches to relate the amide I bands of polypeptides to protein structure have been explored in detail, including normal-mode analysis,[21] coupled oscillator models,[22,23] and ab initio calculations.[24−26]

Recently, it has been shown that two isotope-edited functional groups may interact, which leads to a distance-dependent level splitting characteristic for intraprotein contacts[27,28] or secondary structure elements.[26,28] In this work, we suggest to use this effect to obtain detailed information about the secondary and tertiary structure of homodimers using an even simpler substitution pattern. As an example for the possible detection and characterization of protein−protein interaction, we use the ion channel formed by the Gramicidin A dimer, whose biologically active secondary and tertiary structure has been fiercely disputed.

2. Model

In our work, we focus on the amide I band, which is located in the spectral range between 1600 and 1700 cm^{-1}. It is mainly attributed to C═O band stretching, and due to a large transition dipole moment, it shows a high intensity. As we plan to compute the spectral properties of comparatively large molecules, we rely on an empirical dipole coupling model that has been introduced by Krimm and co-workers.[29] Originally designed to describe the vibrational spectrum of β-sheets, this model has been extended by Torii and Tasumi to simulate other protein secondary structure elements as well.[30] We note that the protein dimer that we plan to study here contains ∼550 atoms and is therefore too large to be treated as a whole by ab initio quantum chemical calculations accurate enough to predict vibrational frequencies. As we are interested in vibrational coupling and decoupling phenomena throughout the entire dimer, all constituents have to treated on an equal footing, thus excluding a combined quantum mechanical−molecular mechanics (QM/MM) approach.

Whereas we rely on a well-tested empirical dipole coupling model here, similar information about peptide vibrational bands can be obtained from a normal-mode analysis, involving either classical force fields[27] or quantum chemical calculations, the latter briefly described below. In either case, the amide I C═O oscillations can be clearly identified, and the corresponding normal modes show weak contributions of CNH and CCH bending, which give rise to the effective mass corrections discussed below. From our experience, the transition dipole coupling (TDC) model used here provides a better description of the amide I band details, which are related to the protein's secondary structure. Furthermore, the TDC model can be applied without performing a full geometry optimization, as (at least

* Corresponding author. E-mail: Thorsten.Koslowski@physchem.uni-freiburg.de.

10.1021/jp053487c CCC: $30.25
Published on Web 11/19/2005

formally) required for a complete normal-mode analysis via the computation of the Hessian matrix.

Within the so-called transition dipole coupling model, the peptide bond dipoles $\vec{\mu}_i$ are mainly oriented along the C═O bond and interact by a potential that depends on the distance r and the orientation of the dipoles:

$$V_{ij} = \frac{e^2}{4\pi\epsilon\epsilon_0}\left(\frac{\langle\vec{\mu}_i|\vec{\mu}_j\rangle}{r_{ij}^{\,3}} - 3\,\frac{\langle\vec{\mu}_i|\vec{r}_{ij}\rangle\langle\vec{\mu}_j|\vec{r}_{ij}\rangle}{r_{ij}^{\,5}}\right) \qquad (2.1)$$

Here, we use the standard parameters of a dipole strength of 3.70 D and an ϵ of unity. The calculation of the vibrational frequencies requires the computation of the eigenvalues of the Hessian matrix **F**, i.e., the matrix of the mixed mass-weighted second derivatives of the potential energy with respect to the coordinates.[31,32] We use a single internal coordinate per oscillator, x_i, which points along the C═O bond, and write the matrix elements as

$$f_{ij} = (m_i m_j)^{-1/2}\,\frac{\partial^2 V}{\partial x_i\,\partial x_j} \qquad (2.2)$$

The solution of the associated eigenvalue problem for N oscillators

$$(\mathbf{F} - \nu^2\mathbf{G})\vec{q} = \vec{0} \qquad (2.3)$$

leads to the frequencies ν_α (or wavenumbers $\tilde{\nu}_\alpha$) and the corresponding eigenvectors $\vec{q}_\alpha$. Within the TDC model, the matrix **G** is set equal to the unit matrix. The infrared intensity for a line $\tilde{\nu}_\alpha$ can be estimated using the eigenvectors and the orientation of the dipoles:

$$I_\alpha \sim \Big(\sum_i q_{i\alpha}[\mu_{ix} + \mu_{iy} + \mu_{iz}]\Big)^2 \qquad (2.4)$$

The right-hand side of eq 2.2 depends on the effective oscillator masses via the prefactor of the partial derivative. Elementary matrix theory suggests a red shift of the frequencies upon the introduction of a single heavier isotope, e.g., the substitution of ^{12}C by ^{13}C or of ^{16}O by ^{18}O, and the normal modes $\vec{q}_\alpha$ tend toward a stronger degree of localization than their isotopically pure counterparts. In a simple *Ansatz*, the elements of the Hessian matrix are rescaled by the ratio of the corresponding reduced oscillator masses. As the oscillators do not consist of isolated C═O groups, but interact with the protein backbone, corrections to this scaling factor may be required. We have performed semiempirical calculations of the isotope-edited vibrations of a Gly_{10} α-helix on the AM1 level[33] using the Gaussian 03 program package[34] to estimate these deviations. They are small and amount to a factor of 0.9950 for carbon and 1.0115 for oxygen isotope substitution. Consequently, isotope shifts are reduced for an ^{18}O substitution compared to the value deduced from the C═O effective mass, and the ^{13}C shift is enhanced as compared to an ideal two-site C═O oscillator. Although the increase of two atomic mass units obtained by substituting ^{16}O by ^{18}O usually suggests a stronger shift than the substitution of ^{12}C by its ^{13}C counterpart, this effect is almost compensated by the coupling of the C═O group to the protein backbone.[35] In the absence of vibrational coupling, the TDC model excitations are located at a central wavenumber of $\tilde{\nu} = 1650$ cm^{-1}.[29,30] Using the aforementioned scaling factor, the corresponding ^{13}C isotope-shifted levels lie at 1606 cm^{-1}.

Recent ab initio calculations by Huang et al. have been devoted to the comparison of ab initio results for doubly substituted ^{13}C═O oscillator level splittings within α-helices to the TDC model predictions.[26] For the ab initio results, the total amide I spectrum is shifted by ∼50 cm^{-1} compared to the experiment. Nevertheless, the results allow a quantitative comparison of the quantum mechanical and the TDC couplings, which roughly converge at oscillator separations larger than 5 Å and which differ by a factor significantly larger than two only for second-nearest-neighbor isotope substitutions at smaller distances.

3. Results and Discussion

In recent work, we have computed the impact of site-specific single and double ^{18}O isotope substitutions within C_α═O bonds upon the infrared spectra of proteins.[28] Compared to the isotopically pure polypeptides, an impurity level can be observed at the low-energy edge of the amide I band. The effect of a double substitution is, however, not simply additive: depending upon the distance and the relative orientation of the isotope-edited dipoles, the two impurity levels couple, and they exhibit an additional spectral splitting. Once the spatial localization of the ^{13}C═O vibrations is strong—a conjecture that will be verified below—the coupling can be described within a simple two-oscillator model.[27] The eigenvalue equation (2.3) turns into the 2×2 problem

$$\begin{pmatrix} \nu_0^{\,2} - \nu^2 & f \\ f & \nu_0^{\,2} - \nu^2 \end{pmatrix}\begin{pmatrix} q_1 \\ q_2 \end{pmatrix} = \vec{0} \qquad (3.1)$$

with distance- and orientation-dependent coupling constants f (eq 2.2) and the isotope-shifted central frequency of the TDC model, ν_0. As a solution of the problem (3.1), we obtain two frequencies, which can be characterized by a level splitting of $\Delta\nu = \sqrt{2f}$ that serves as the measurable quantity associated with the strength of interaction between two C═O groups. These groups interact once they are neighbors in space, but not necessarily in sequence. As a consequence, double isotope substitution may serve as a tool to obtain structural information about proteins which are difficult to crystallize. In addition, typical secondary structure elements are manifest as characteristic fingerprints in the strength of the level splitting as a function of the two indices of the isotope-edited amino acids.[28] For single-isotope levels entering the diagonal of the secular matrix of eq 3.1 with different ν_0 values, the results obtained from an analysis similar to the one just performed does not lead to qualitative differences.[27] The intensities of the two split impurity are sensitive to the relative orientation of the two coupled C═O oscillators, with the extreme of one vanishing line in an arrangement where the two dipoles are collinear.

It is evident that this technique is by no means limited to the detection of intraprotein contacts but may also be applied to protein−protein interactions. Here, we address the question of the impact of dimerization upon the IR spectra of proteins. As a model system, we use Gramicidin A from *Bacillus brevis*, a small polypetide consisting of 15 amino acids with the sequence For-VGALAVVVWLWLWLW-Eta. Because of the presence of the amino acids D-Leu (positions 4, 10, 12, and 14) and D-Val (positions 6 and 8), Gramicidin A forms a right-handed β-helix. The biopolymer dimer is classified as an ion-channel membrane protein; in this function, it also acts as an antibiotic. The polypetide easily undergoes a dimerization reaction, and it exhibits an interesting polymorphism. In oriented bilayers, the two helices show a head-to-head configuration with respect to their amino acid sequences (protein database code 1MAG[36]), as depicted in Figure 1a. In the bulk phase, a structure of two

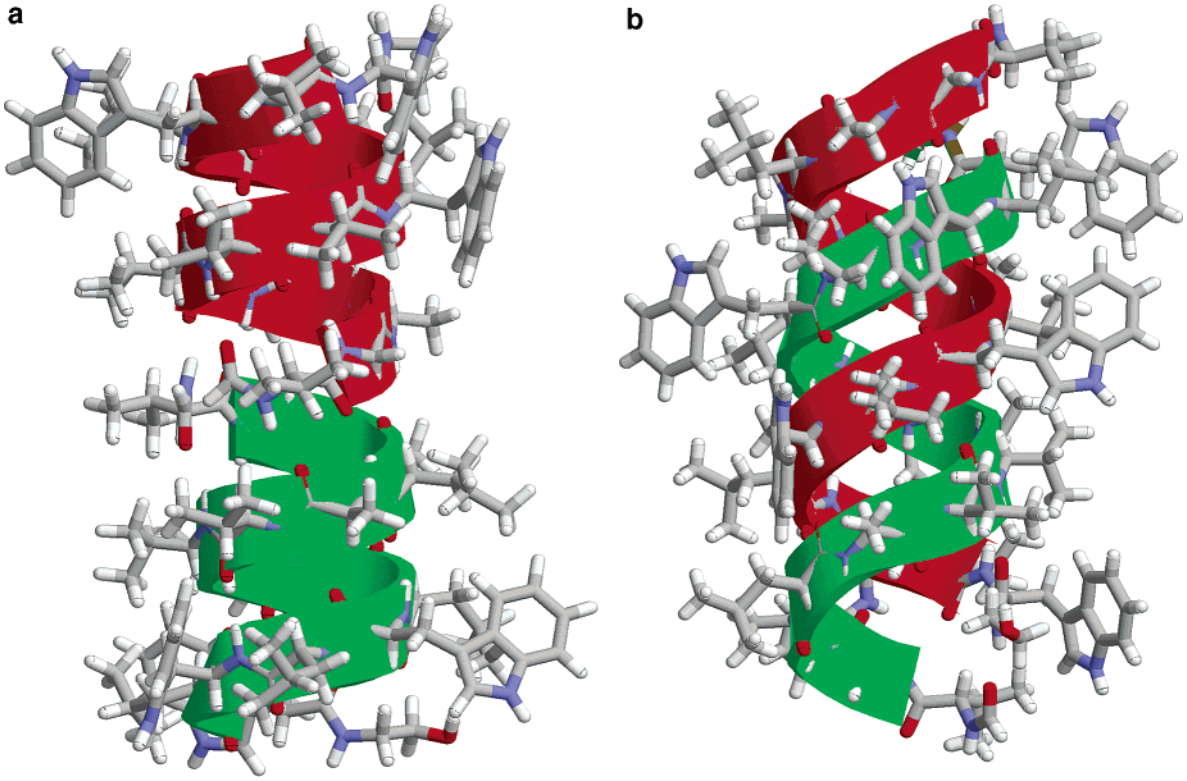

Figure 1. Cartoon models of two polymorphs of the Gramicidin A dimer: (a) head-to-head contact (protein database file 1MAG[36]) and (b) double-helix (protein database file 1AV2[37]).

antiparallely oriented chains that form a double helix has been determined (protein database code 1AV2[37]), which is depicted in Figure 1b. For convenience, we will refer to these structures as the head-to-head (H2H) and the double-helix (DH) form.

We now turn the computation of the IR spectra of the H2H and the DH form. Within the TDC model, the unsubstituted spectra lie in the typical amide I band range between ~1600 and ~1700 cm^{-1}. The spectra exhibit a peak at ~1625 cm^{-1}, which has its origin rather in the high intensity of the vibrational lines in the red part of the spectrum rather than a high vibrational density of states. With increasing wavenumber, the intensity falls off. For H2H, the high-energy part of the spectrum exhibits two additional small maxima, whereas the DH spectrum in this region is featureless. The H2H spectrum is shown in Figure 2a.

For proteins that form a homodimer, it is not possible to selectively substitute an amino acid in only one of the monomers. Thus, a well-defined singly substituted reference spectrum is not available. We therefore suggest a different strategy to identify the level splitting: we simulate a concentration series with x as the fraction of polypeptides that have a specific backbone $^{12}C_\alpha$ carbon atom substituted by a $^{13}C_\alpha$. If all monomers form dimers and if there is no interaction between the dimers, we will observe spectra due to the formation of dimers consisting of zero, one, or two ^{13}C-edited partners with intensities $I_0(\tilde{\nu})$, $I_1(\tilde{\nu})$, and $I_2(\tilde{\nu})$, as shown in Figure 2b. At different isotope concentrations $0 < x < 1$, the total spectrum will show contributions arising from all of these configurations. For small nonzero values of x, completely unsubstituted dimers will dominate the spectrum, with a small fraction of aggregates that contain an edited and an unsubstituted monomer. The fraction of the latter will increase with increasing x, until for large isotope concentrations, both monomers that constitute a dimer are very likely to contain a ^{13}C atom at a specific position i. The probability of finding a dimer that is formed by two,

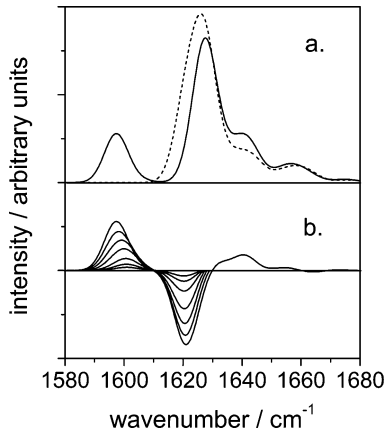

Figure 2. Computed infrared spectra of substituted Gramicidin A dimers: (a) dotted line, unsubstituted amide I band; solid line, ^{13}C Val3-substituted spectrum. (b) Difference spectra for isotope concentrations of 0.05, 0.1, 0.2, 0.4, 0.6, 0.8, and 1.0, left peak from bottom to top, right peak from top to bottom. Above $\tilde{\nu} = 1630$ cm^{-1}, only the fully substituted spectrum is shown for convenience. All spectral lines have been broadened by a Gaussian function with a rmsd parameter of 4.0 cm^{-1}. The intensity scales used in (a) and (b) are identical.

one, or no isotope-edited monomers is given by elementary statistics as x^2, $2x(1-x)$, and $(1-x)^2$, respectively. We thus have an observable sum spectrum

$$I_S(\tilde{\nu}) = x^2 I_2(\tilde{\nu}) + 2x(1-x)I_1(\tilde{\nu}) + (1-x)^2 I_0(\tilde{\nu}) \quad (3.2)$$

To enhance the spectral changes induced by isotope editing, it is a common practice to make use of a so-called difference spectrum

$$\Delta I(\tilde{\nu}) = I_S(\tilde{\nu}) - I_0(\tilde{\nu}) \quad (3.3)$$

Computed $\Delta I(\tilde{\nu})$ spectra are shown in Figure 2b for a H2H Val3

$^{13}C_\alpha$ isotope substitution at $x = 0.05$, 0.1, 0.2, 0.4, 0.6, 0.8, and 1.0. At small x, we note a peak in the low-energy part of the difference spectra centered at 1601.1 cm^{-1}. With increasing x, it is gradually shifted to the red, until for complete isotope substitution, a value of $\tilde{\nu} = 1597.3$ cm^{-1} emerges. This shift of 3.8 cm^{-1} can be traced back to the coupling of isotope impurity levels—as discussed above—and is equivalent to a spectral coupling of $\Delta\tilde{\nu} = 7.6$ cm^{-1}. Because of the parallel arrangement of the Val3 amino acids in the H2H configuration of the Gramicidin A dimer, the second, blue-shifted peak at $\tilde{\nu} = 1605.0$ cm^{-1} has an almost vanishing intensity and does not show up in the spectrum as an individual peak. Around $\tilde{\nu} \simeq 1620$ cm^{-1}, the difference spectrum is negative, thus indicating that the buildup of the intensity within the impurity bands is formed at the expense of the intensity at the low-energy part of the unedited spectrum. A corresponding isosbestic point at $\tilde{\nu} \simeq 1610$ cm^{-1} can be observed. We note that for a concentration series eq 3.2 leads to a system of equations from which the individual spectra $I_0(\tilde{\nu})$, $I_1(\tilde{\nu})$, and $I_2(\tilde{\nu})$ can be extracted.

Above, the coupling and splitting of isotope impurity levels are described within a simple two-oscillator model that relies on spatial localization upon the introduction of a single substitution. As a standard measure of localization, we use the participation ratio of an eigenvector (or generalized coordinate) $\vec{q}_\alpha$ corresponding to a wavenumber $\tilde{\nu}_\alpha$ to verify this assumption. For a normalized eigenvector, the inverse participation ratio is given by[38]

$$P_\alpha^{-1} = \sum_i q_{i\alpha}^4 \tag{3.4}$$

P_α is usually interpreted as the number of sites that participate in an elementary excitation,[39] as evident from its limiting behavior in the case of complete localization ($P_\alpha = 1$) and uniform delocalization ($P_\alpha = N$). For the spectra shown in Figure 2b, we have $P_1 = 1.4$ for a single isotope substitution, which is observable around 1601 cm^{-1}. This implies that the corresponding vibrational excitation is strongly localized and essentially confined to the ^{13}C-edited oscillator. $^{12}C{=}O$ Gramicidin vibrations, on the other hand, are characterized by P_α values ranging from ∼6 to ∼18. For doubly substituted systems, the localized isotope-edited oscillators couple and give rise to a combined symmetric and a corresponding antisymmetric mode. For systems that are close to the two-oscillator ideal, this coupling induces a participation of two isotope-edited oscillators; hence, the participation ratio is supposed to be doubled here. We indeed compute $P_1 = P_2 = 2.8$ for a ^{13}C Val 3 double substitution, which strongly indicates that the assumptions underlying the two-oscillator model are essentially valid. We note that the two-oscillator model is only used as a simple frame to rationalize findings like impurity level formation and splitting, whereas a quantitative analysis always makes use of the TDC model, as described and referenced above. The strong localization of $^{13}C{=}O$ impurity levels has also been attested by Huang et al. within their ab initio and TDC model calculations of spectral couplings within α-helices.[26]

We now turn to the computation of the spectral splittings $\Delta\tilde{\nu}$ for the H2H and the DH arrangement of Gramicidin A dimers. In Figure 3, the level splitting for the H2H configuration is shown as a function of the sequence number of the substituted amino acid i. As an overall trend, we note that the level splitting decreases with decreasing i, a fact that would indeed suggest a head-to-head arrangement of two entities within a dimer. Pronounced peaks in $\Delta\tilde{\nu}(i)$ can be observed at $i = 3$ ($\Delta\tilde{\nu} = 7.6$ cm^{-1}), $i = 9$ ($\Delta\tilde{\nu} = 4.2$ cm^{-1}), and $i = 15$ ($\Delta\tilde{\nu} = 1.6$ cm^{-1}).

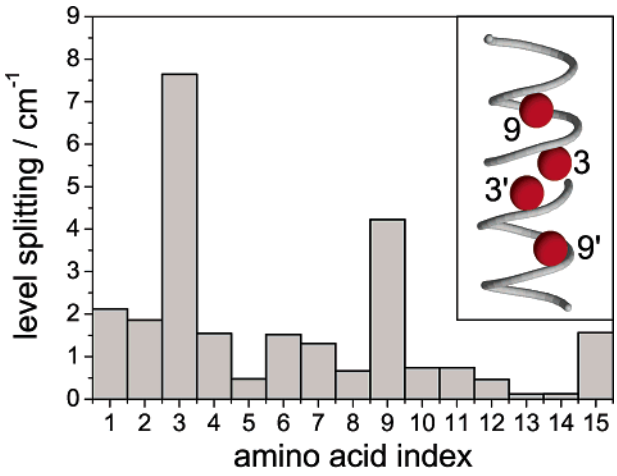

Figure 3. Infrared level splitting of a head-to-head Gramicidin A dimer as a function of the substituted monomer amino acid. The dimer conformation and two substitution patterns that give rise to a large splitting are shown in the inset.

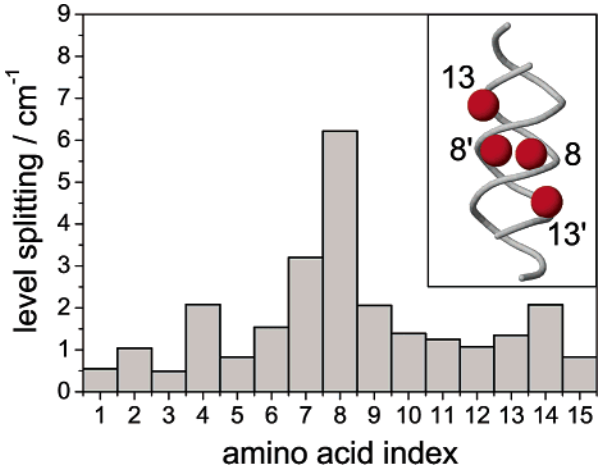

Figure 4. Infrared level splitting of a double-helix Gramicidin A dimer as a function of the substituted monomer amino acid. The dimer conformation and two substitution patterns are shown in the inset.

They reflect the structure of the β-helix with a periodicity of ∼6. In terms of the resolution of difference spectra, the first two of these patterns should be clearly observable. The intensities of the Val3 oscillators, which exhibit the highest coupling, are almost collinear and point toward each other, as deducible from the vanishing high-energy line upon coupling (cf. Figure 2b). In contrast to the H2H arrangement, the corresponding dependence of $\Delta\tilde{\nu}$ upon i for the double-helical conformation—as displayed in Figure 4—exhibits a single peak at $i = 8$. This would suggest a contact of the two Gramicidin A monomers only close to their respective centers, a picture that is consistent with an antiparallel arrangement of the subunits. Comparing Figures 3 and 4, it is evident that H2H and DH conformers show level splitting patterns that can be clearly distinguished, even considering the recently reported possible deficiencies of the TDC model at small oscillator distances.[26] Consequently, it is feasible to obtain the overall geometric features of the dimers from these plots.

It is worthwhile to compare our method with three-dimensional NMR spectroscopy. By using the nuclear Overhauser effect, through-space interactions can be analyzed providing distant-dependent information between two amino acid residues. However, this method is limited to distances below 5 Å and proteins with a molecular weight of less than 30 000 Da.[40] In addition, the spectra may be difficult to interpret in

metalloproteins as the paramagnetic atoms/ions broaden the NMR signals. A big advantage of the infrared spectroscopy is the small amount of sample needed which is approximately a factor 100 less than for an NMR experiment. Therefore, we conclude that isotope-edited infrared spectroscopy may be a powerful tool, especially in cases where only distance information between two distinct residues is required rather than a complete three-dimensional structure. Moreover, the method allows very high time resolution for investigating the dynamics of labeled intermediates.

4. Conclusions

Focusing on the Gramicidin A polypeptide, we have studied the impact of the tertiary structure of the respective dimers upon the isotope-edited infrared difference spectra. As a computational scheme, we have used an empirical dipole coupling model adequate to the description of the amide I band. We find the usual spectral patterns of protein isotope substitution spectroscopy:[27,28] applying a single substitution within a C_α═O oscillator using a heavy isotope, a single red-shifted localized impurity level is split from the bulk of the spectrum. If two peptide bonds are edited, the corresponding oscillators will couple, which gives rise to a splitting of the impurity levels. This level splitting depends on the distance and the relative orientation of the participating oscillators. Consequently, the knowledge of its magnitude is tantamount to a piece of information about the local geometry of a system.

For homodimerization, it is sufficient to substitute a single amino acid within each polypeptide monomer to observe the aforementioned level splitting. The problem of obtaining a singly substituted reference spectrum can be circumnavigated by recording IR spectra for a series of concentrations with a different isotope content. We have computed level splittings as a function of the substituted amino acid's index for two different spatial arrangements of Gramicidin A dimers, which show characteristic fingerprints of the head-to-head or double-helix arrangements. Besides detecting protein dimers possible applications of this method include the identification of key residues involved in enzyme catalysis or the analysis of protein−ligand interactions.

We are aware of the fact that the preparation of ^{13}C═O-labeled proteins is costly and time-consuming, which will certainly not permit the application of isotope-edited vibrational coupling spectroscopy as a routine method for protein structure analysis. Efforts involving a similar amount of preparative work are, however, not uncommon in obtaining structural information about proteins and their aggregates. As a recent example, we refer to three approaches to the structure and dynamics of yeast amyloid fibrils, which have been motivated by getting insight into the microscopic mechanism of prion-induced diseases.[41−43] Of these, the work of Krishnan and Lindquist[42]—coined as heroic in a review[44]—has involved the generation of 1629 cystein mutants to provide binding sites for fluoresence labels with varying distances.

In our work, we hope to have demonstrated that a few strategically selected labels can be sufficient to verify or falsify a structure, in particular if homodimers are concerned. The corresponding labeled amino acids are commercially available due to the demand of protein NMR spectroscopists,[45] and as shown above, the labeling does not necessarily have to be complete, leading to a further reduction in costs.

Acknowledgment. It is a pleasure to thank P. Gräber and C. A. Zell for fruitful discussions and helpful comments.

References and Notes

(1) Winter, R.; Nöll, F. *Methoden der Biophysikalischen Chemie*; Teubner: Stuttgart, 1989; p 359.
(2) Chin, J. K.; Jimenez, R.; Romesberg, F. E. *J. Am. Chem. Soc.* **2001**, *123*, 2426.
(3) Torres, J.; Kukol, A.; Arkin, I. T. *Biophys. J.* **2000**, *79*, 3139.
(4) Torres, J.; Arkin, I. T. *Biophys. J.* **2002**, *82*, 1068.
(5) Sonar, S.; Lee, C. P.; Coleman, M.; Patel, N.; Liu, X.; Marti, T.; Khorana, G. H.; RajBhandary, U. L.; Rothschild, K. J. *Nat. Struct. Biol.* **1994**, *1*, 512.
(6) Bergo, V.; Mamaev, S.; Olejnik, J.; Rothschild, K. J. *Biophys. J.* **2003**, *84*, 960.
(7) Siebert, F.; Mäntele, W. *Eur. J. Biochem.* **1983**, *130*, 565. Arrondo, J. L. R.; Muga, A.; Castresana, J.; Goni, F. M. *Prog. Biophys. Mol. Biol.* **1993**, *59*, 23.
(8) Chin, J. K.; Jimenez, R.; Romesberg, F. E. *J. Am. Chem. Soc.* **2002**, *124*, 1846.
(9) Ohno, K.; Nomura, S.; Yoshida, H.; Matsuura, H. *Spectrochim. Acta A* **1999**, *55*, 2231.
(10) Grajcar, L.; Baron, M. H.; Becouran, S.; Czernecki, S.; Valery, J. M.; Reiss, C. *Spectrochim. Acta A* **1994**, *50*, 1015.
(11) Dluhy, R. A.; Mendelsohn, R.; Casal, H. L.; Mantsch, H. H. *Biochemistry* **1983**, *22*, 1170.
(12) Pastrana, B.; Mautone, A. J.; Mendelsohn, R. *Biochemistry* **1991**, *30*, 10058.
(13) Echabe, I.; Requero, M. A.; Goni, F. M.; Arrondo, J. L. R.; Alonso, A. *Eur. J. Biochem.* **1995**, *231*, 199.
(14) Fraile, M. V.; Lopez-Rodriguez, G.; Gallego-Nicasio, J.; Carmona, P. *Biopolymers* **2000**, *57*, 11.
(15) Silva, R. A. G. D.; Kubelka, J.; Bour, P.; Decatur, S. M.; Keiderling, T. A. *Proc. Natl. Acad. Sci. U.S.A.* **2000**, *97*, 8318.
(16) Moritz, R.; Fabian, H.; Hahn, U.; Diem, M.; Naumann, D. *J. Am. Chem. Soc.* **2002**, *124*, 6259.
(17) Silva, R. A. G. D.; Nguyen, J. Y.; Decatur, S. M. *Biochemistry* **2002**, *41*, 15296.
(18) Barber-Armstrong, W.; Donaldson, T.; Wijesooriya, H.; Silva, R. A. G. D.; Decatur, S. M. *J. Am. Chem. Soc.* **2004** *126*, 2339.
(19) Silva, R. A. G. D.; Barber-Armstrong, W.; Decatur, S. M. *J. Am. Chem. Soc.* **2003**, *125*, 13674.
(20) Bredenbeck, J.; Helbing, J.; Kumita, J. R.; Woolley, G. A.; Hamm, P. *Proc. Natl. Acad. Sci. U.S.A.* **2005**, *102*, 2379.
(21) Krimm, S.; Bandekar, J. *Adv. Protein Chem.* **1986**, *38*, 181.
(22) Lee, S. H.; Krimm, S. *Chem. Phys.* **1998**, *230*, 277.
(23) Brauner, J. W.; Flach, C. R.; Mendelsohn, R. *J. Am. Chem. Soc.* **2005**, *127*, 100.
(24) Bour, P.; Kubelka, J.; Keiderling, T. A. *Biopolymers* **2002**, *65*, 45.
(25) Silva, R. A. G. D.; Kubelka, J.; Decatur, S. M.; Bour, P.; Keiderling, T. A. *Proc. Natl. Acad. Sci. U.S.A.* **2000**, *97*, 8318.
(26) Huang, R.; Kubelka, J.; Barber-Armstrong, W.; Silva, R. A. G. D.; Decatur, S. M.; Keiderling, T. A. *J. Am. Chem. Soc.* **2004**, *126*, 2346.
(27) Becker, J.; Becher, F.; Hucke, O.; Labahn, A.; Koslowski, T. *J. Phys. Chem. B* **2003**, *107*, 12878.
(28) Koslowski, T.; Labahn, A. *ChemPhysChem* **2004**, *5*, 233.
(29) Moore, W. H.; Krimm, S. *Proc. Natl. Acad. Sci. U.S.A.* **1975**, *72*, 4933. Krimm, S.; Abe, Y. *Proc. Natl. Acad. Sci. U.S.A.* **1972**, *69*, 2788.
(30) Torii, H.; Tasumi, M. *J. Chem. Phys.* **1992**, *96*, 3379.
(31) Wilson, E. B., Jr.; Decius, J. C.; Cross, P. C. *Molecular Vibrations*; Dover Publications: New York, 1955.
(32) Madelung, O. *Festkörpertheorie I*; Springer Verlag Heidelberger Taschenbücher: Heidelberg, 1972.
(33) Dewar, M. J. S.; Zoebisch, E. G.; Healy, E. F.; Stewart, J. J. P. *J. Am. Chem. Soc.* **1985**, *107*, 3902.
(34) Gaussian 03: Frisch, M. J., et al. Gaussian Inc., Pittsburgh, PA, 2003.
(35) Zehender, F., unpublished results.
(36) Ketchem, R. R.; Lee, K. C.; Huo, S.; Cross, T. A. *J. Biomol. NMR* **1996**, *8*, 1. Hu, W.; Lazo, N. D.; Cross, T. A. *Biochemistry* **1995**, *34*, 14138. Ketchem, R. R.; Hu, W.; Cross, T. A. *Science* **1993**, *261*, 1457.
(37) Burkhart, B. M.; Li, N.; Langs, D. A.; Pangborn, W. A.; Duax, W. L. *Proc. Natl. Acad. Sci. U.S.A.* **1998**, *95*, 12950.
(38) Bell, R. J.; Dean, P. *Disc. Faraday Soc.* **1970**, *50*, 55.
(39) Thouless, D. J. *Phys. Rep.* **1974**, *13*, 93.
(40) Wright, P. E. *Trends Biochem. Sci.* **1989**, *14*, 255.
(41) Nelson, R.; Sawaya, M. R.; Balbirnie, M.; Madsen, A. Ø.; Riekel, C.; Grothe, R.; Eisenberg, D. *Nature (London)* **2005**, *435*, 773.
(42) Krishnan, R.; Lindquist, S. L. *Nature (London)* **2005**, *435*, 765.
(43) Ritter, C.; Maddelein, M.-L.; Siemer, A. B.; Lührs, T.; Ernst, M.; Meier, B. H.; Saupe, S. J.; Riek, R. *Nature (London)* **2005**, *435*, 844.
(44) Dobson, C. M. *Nature (London)* **2005**, *435*, 747.
(45) Cambridge Isotopes Laboratories, private communication.